

# Do the Large Magellanic Cloud and the Milky Way Globular Clusters Share a Common Origin?

B.E. Tucker<sup>1,2</sup>  
*Department of Physics*  
*University of Notre Dame*  
btucker2@nd.edu

Advised by: K.Olsen and B.Blum  
*Astronomers, Cerro Tololo Inter-American Observatory Casilla 603 La Serena, Chile*

## ABSTRACT

We took infrared spectroscopy in the wavelength of  $1.5552\mu m$  and  $1.5600\mu m$ , of six metal poor red giant stars in NGC 2019 with the Phoenix high-resolution spectrograph at the 8.1 Geminin South telescope. Previous measurements and calculations of NGC 2019 have metallicities differing by .6dex and age within 1 Gyr of the oldest globular clusters in the Milky Way. We carried out detailed analysis on the six stars in order to determine accurate oxygen and iron abundances to see if a similarities exist between the LMC and the Milky Way globular clusters. We calculated, through different methods, the stellar parameters of effective temperature, bolometric correction, gravity, luminosity, and microturbulent velocity. We calculated these in order to accurately obtain stellar atmosphere models. The model atmosphere that we used, produced strong and dispersed [Si/Fe] and [Ti/Fe] due to the strong impact of the microturbulent velocity. We calculated a mean Oxygen to Iron ratio of .35, which is similar but not the same as that found in the Milky Way.

## 1. Introduction

The question of whether the Milky Way Galaxy Globular Clusters share a same parent population with those in the Large Magellanic Cloud (LMC) is a very interesting one and one that would provide insight into galaxy formation. Globular clusters are home to some of the first stars to form and are some of the oldest objects in the Universe, with some, like NGC 2019 dating about 12 billion years. Also, the LMC is a much smaller galaxy than the Milky Way. If the results show that indeed, the globular clusters in both the LMC and Milky Way have similar metallicities, than

that could mean that galaxies like the Milky Way, who collide and combine with smaller galaxies, like the LMC, were formed around at the same time. Galaxy formation is one of the big questions in Astronomy and so determining where the globular clusters in the LMC and the Milky Way are the same, can provide new information on this topic.

Studies using the Hubble Space Telescope (HST) of the LMC's globular cluster system have suggested they could have been drawn from the same parent population as those in our galaxy due to similar measurements of ages and bulk metallicities. Thus, thorough observations of the LMC are needed in order to solve this question.

Six stars in the LMC globular cluster NGC 2019 were chosen to be studied. However, as of now, the only current measurements of NGC 2019 are using low resolution Ca- triplet spectroscopy and isochrone fitting disagree over  $[Fe/H]$ . Since

---

<sup>1</sup>Project conducted while a participant in the 2006 Cerro Tololo Inter-American Observatory Research Experience for Undergraduates (REU) Program, funded for by the National Science Foundation (NSF)

<sup>2</sup>Address: 225 Nieuwland Science Hall Notre Dame, IN 46556 USA

globular clusters are sensitive to both oxygen and iron, high resolution spectroscopy is needed. Previous studies of NGC 2210, another globular cluster in the LMC revealed a low oxygen abundance, and so measuring accurately more stars in the LMC is particularly interesting.

## 2. Observations

### 2.1. Data

The data for this project was taken on the Gemini South Observatory, operated and run by the Association of Universities for Research in Astronomy (AURA). High resolution infrared spectra was taken using the Phoenix spectrograph in the wavelength range of  $1.5552\mu m$  and  $1.5600\mu m$ .

Five nights of data were taken in April of 2002. The stars observed were six metal poor red giant stars in NGC 2019. Infrared spectra was also taken of HD 32440 in order to be used for wavelength calibration.

Since the six stars in this project were hot, red giant stars, they were featureless and thus the telluric absorption did not affect the spectroscopic measurements.

### 2.2. Data Reduction

The data was reduced following the standard Phoenix procedures.

The trim section for all of the data was [14:226,65:1024] using the CCDPROC feature in CCDRED package of the IMRED package of the Image Reduction and Analysis Facility (IRAF) program, thus removing the pixels present that had flawed or unusable data. The flat field and dark frames were combined. The flat field and dark frames were combined using the standard tasks of DARKCOMBINE and FLATCOMBINE in the same package as CCDPROC. One remark is that no dark or flat frames were taken, or at least were saved and recorded, on the second night of observing, so the flat field and dark frames from the first night were used for the second night.

The next step taken was to further prepare the flat field frames. The combined dark frames were subtracted from the combined flat fields and then normalized using the median of each frame. A response image was creating by making a fit to the normalized frame using the RESPONSE task in

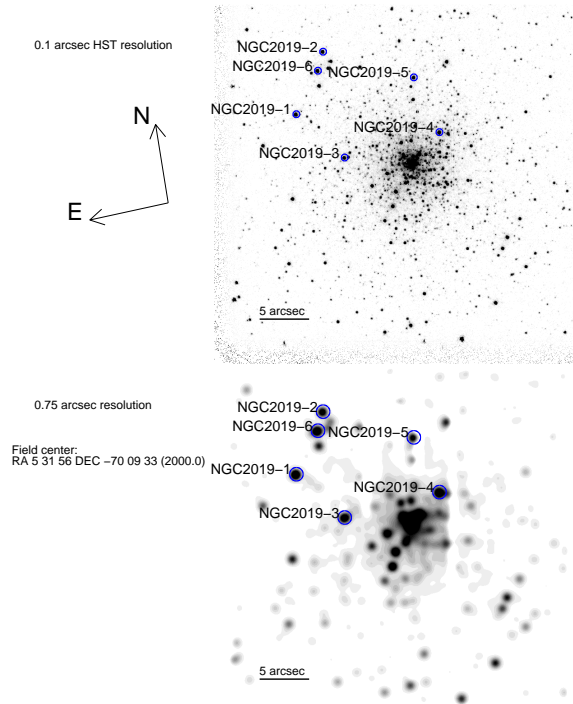


Fig. 1.— Visual of images of the six target stars in NGC 2019

TABLE 1  
TARGET STARS

Star	RA	Dec
NGC2019-1	05:31:57.8624	-70:09:31.0199
NGC2019-2	05:31:55.9146	-70:09:30.8929
NGC2019-3	05:31:58.5803	-70:09:25.5760
NGC2019-4	05:31:56.1399	-70:09:24.8940
NGC2019-5	05:31:57.9520	-70:09:21.8541
NGC2019-6	05:31:57.7599	-70:09:20.1189

TABLE 2  
MEDIAN VALUES OF EACH NIGHT OF DATA

Night	Median
Night 1	1479
Night 2	1479
Night 3	1484
Night 4	1485
Night 5	1484

the TWODSPEC LONGSLIT package. For the response fitting, a restriction of [49:168,65:1024] was used in order to use only the part of the spectrograph that was illuminated.

The images were then subtracted by pairs and then normalized by the RESPONSE image. In order to do this, the images were sorted according to the object of which the spectra was taken, since subtracting different stars would give very different results. The APALL task in the APEXTRACT package was used to extract the one dimensional spectrum of the star in each of the normalized subtracted images. During the extraction process, the background subtraction was fit individually so as to make sure the appropriate background was eliminated while not eliminating the star. Using the CONTINUUM task, a continuum was fit to each extracted spectrum in order to fit the spectra to a value of one to eliminate distortion in the absorption lines.

The wavelength calibration was done using the spectra taken from HD 32440, a K4 III spectral type star, which was observed and measured on every night data was taken. Using the Infrared Atlas

of the Arcturus Spectrum of  $0.9-5.3\mu\text{m}$  by Hinkle, Wallace, and Livingston, the lines were identified in the star. Using the calibrated spectrum, all of the images were edited with this calibration using DISPCOR by editing the files using REFSPEC1. The stars were then combined using SCOMBINE, creating one normalized, reduced spectra for each of the six NGC 2019 stars that were observed.

Upon the stars being combined, each combined spectrum was again fit with a continuum of one in the same process as in each individual star. This was done in order to fix a slump that was present at the end of the spectrum in each of the six stars. After this was done, a velocity correction was needed of each star. Using a sample spectrum from Melendez, Barbuy, and Spite (2001) the strong lines that were present in the data were identified in the Melendez, Barbuy, and Spite sample spectrum. The shift of the observed lines was then calculated from the actual lines for each line in each star. The overall average redshift was computed for the six stars.

TABLE 3  
WAVELENGTH CALIBRATION LINES

Wavelength	Element
15544.85	Ni
15546.33	Fe
15548.00	Ti
15554.70	Fe
15555.68	Fe
15559.62	Ni
15562.04	Si
15564.50	OH
15567.61	CN
15573.04	OH
15576.34	OH
15580.60	CN
15585.02	CN
15592.52	Fe
15594.31	Fe
15595.75	Fe
15598.01	Fe

### 3. Analysis

In order to properly analyze the chemical abundances of the six stars, the stellar parameters of effective temperature, bolometric correction, luminosity, gravity, and microturbulent velocity were needed in order to obtain the correct model atmospheres.

#### 3.1. Effective Temperature

V band and I band photometry was taken of each object. Subtracting the I band photometry from the V band and subtracting a value of .078,

$$(V - I) - .078 = (V - I)_0 \quad (1)$$

the reddening effect of the inter stellar medium, the appropriate V-I photometry was obtained. Using the relation of effective temperature to the (V-I) photometry from Houdashelt, Bell, and Sweigart (2000)

$$T_{eff} = a + b(color) + c(color)^2 \quad (2)$$

where a has a value of 8556.22, b has a value of -5235.57, and c equaling 1471.09. The data can be

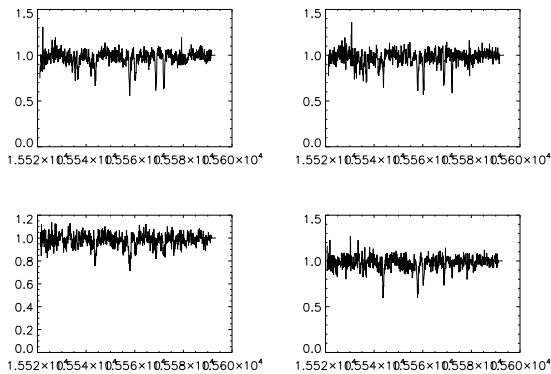


Fig. 2.— Fully reduced spectra of stars 1,3,4,6

TABLE 4  
WAVELENGTH CALIBRATION LINES

Measurement	NGC2019-1	NGC2019-2	NGC2019-3	NGC2019-4	NGC2019-5	NGC2019-6
15572.1	15589.4	15589.5	15589.2	15589.1	15589.0	15589.7
Shift	17.3	17.4	17.1	17.0	16.9	17.6
Velocity	333.28	335.21	329.44	327.51	325.58	339.07
15568.8	15586.1	15586.1	15585.9	15585.9	15585.8	15586.4
Shift	17.3	17.3	17.1	17.1	17.0	17.6
Velocity	333.36	333.36	329.51	329.51	327.58	339.14
15560.3	15577.6	15577.7	15577.4	15577.5	15577.4	15577.9
Shift	17.3	17.4	17.1	17.2	17.1	17.6
Velocity	333.54	335.47	329.69	331.61	329.69	339.33
15557.8	15575.2	15575.2	15575.1	15575.1	15574.9	15575.6
Shift	17.4	17.4	17.3	17.3	17.1	17.8
Velocity	335.52	335.52	333.59	333.59	329.74	343.24
15543.7	15561.1	15561.0	15560.9	15560.8	15560.7	15561.4
Shift	17.4	17.3	17.2	17.1	17.0	17.7
Velocity	335.83	333.90	331.97	330.04	328.11	341.62
15542.1	15559.3	15559.2	15559.0	...	15558.9	15559.5
Shift	17.2	17.1	16.9	...16.8	17.4	
Velocity	332.00	330.07	326.21	...324.28	335.86	
15535.5	15552.8	...	15552.5	...	...	15553.1
Shift	17.3	...	17.0	...	...	17.6
Velocity	334.07	...	328.28	...	...	339.87
15534.2	15551.6	...	15551.3	...	...	15551.9
Shift	17.4	...	17.1	...	...	17.7
Velocity	336.03	...	330.24	...	...	341.83
Average Velocity	334.20	333.98	329.87	330.45	327.50	340.00

TABLE 5  
V BAND AND I BAND PHOTOMETRIC DATA

Star	V Band	Error in V	I Band	Error in I
NGC2019-1	14.8831	.056	16.4651	.042
NGC2019-2	14.6351	.055	16.3150	.041
NGC2019-3	14.5281	.059	16.2481	.050
NGC2019-4	14.9401	.056	16.5060	.047
NGC2019-5	14.6301	.059	16.2510	.114
NGC2019-6	14.9371	.059	16.5501	.049

found in Table 6 of Houdashelt, Bell, and Sweigart (2000), under V-I photometry for Cousins system.

### 3.2. Bolometric Correction

The bolometric correction was obtained by interpolating the calculated effective temperature versus data by Bessel. Using the values for bolometric correction and effective temperature with  $\log g$  values of 0 and .5, the best overall relation to the calculated effective temperatures was made. With this, the most appropriate bolometric correction values were obtained.

### 3.3. Luminosity

In order to calculate the luminosities of the stars, first the absolute magnitude had to be calculated.

$$M_v = V - A_v - (m - M)_o \quad (3)$$

Using the V band to measure the apparent magnitude and along with accounting for the absorption by dust,

$$A_v = 3.1 * (E(V - I)/1.3) \quad (4)$$

where the reddening,  $E(V-I)$  equals .078, a value of .186 for  $A_v$  is obtained. This is along with the distance modulus of the star which is obtained through

$$(m - M)_o = 5 \log d - 5 \quad (5)$$

where  $d$  is the measured distance to the star, and in this case, the star is in the LMC, whose distance is known to be 50.1 kpc, or 4.7 log kpc, gives a distance modulus of 18.5. Using this, the luminosity was obtained. First needed was the bolometric magnitude, which, using the apparent magnitude and the bolometric correction can be obtained using the equation

$$M_v + BC(V) = M_{bol} \quad (6)$$

while the luminosity is related to the bolometric magnitude using

$$M_{bol} = -2.5[\log(L/L_o)] + M_{bol,\odot} \quad (7)$$

where  $M_{bol,\odot}$  is the bolometric magnitude of the sun which is 4.74. Combining all this gives the log of the luminosity.

$$\log(L/L_o) = (M_{bol} - 4.74) / -2.5 \quad (8)$$

### 3.4. Gravity

Using the same Bessel paper from where the bolometric correction interpolation was done, interpolation with isochronic fitting was used to calculate  $\log g$ . Two isochrones with parameters of age, luminosity, and gravity were used to model the parameters of our stars. Using  $\log g$  values of 0 and .5, an age of about 12 Gyr and the calculated luminosities, a plot of  $\log g$  versus  $\log l$  was made. Using the corresponding results of  $\log g$  versus  $\log l$ , isochrones were over plotted against it, and the corresponding values were interpolated in IDL using LINTERP. Upon doing this, the isochrone with the best fit was used as the value for  $\log g$ , which ended up to be .5.

### 3.5. Microturbulent Velocity

The microturbulent velocity was used through interpolation using the isochrones that were used in determining the log of gravity. Plotting the log gravity versus the microturbulent velocities from the isochrones, and then also plotting the bolometric magnitude versus the microturbulent velocities from the isochrones and averaging the corresponding results, the microturbulence was found.

## 4. Abundances

### 4.1. Models

With the parameters obtained from earlier calculations, MARCS models were downloaded from the MARCS website. In all, 8 model atmospheres were analyzed, all being within range of the calculated parameters of temperature, mass, gravity, and velocity, but with some slight, unique variation in one or more of the parameters. Using MOOG, a model atmosphere and abundance analysis program, these were analyzed with the velocity corrected combined spectra of the six stars.

### 4.2. Gaussian Fit

Before the analysis could begin, an appropriate fit of the model to the data was needed.

TABLE 6  
STELLAR PARAMETERS

Star	$V_{I_o}$	$T_{eff}$	$M_v$	BC(V)	Log of Luminosity	Log g	Microturbulent Velocity
NGC2019-1	1.6420	3925.71	-2.4379	-1.22	3.35916	.285267	2.71146
NGC2019-2	1.5350	3985.84	-2.1359	-1.09	3.18636	.465304	2.57865
NGC2019-3	1.5040	4009.55	-2.2209	-1.04	3.20036	.445139	2.58778
NGC2019-4	1.6019	3944.30	-2.3710	-1.18	3.31640	.353549	2.68567
NGC2019-5	1.4915	4022.98	-2.1800	-1.02	3.17600	.480140	2.56554
NGC2019-6	1.5429	3980.25	-2.4350	-1.10	3.31000	.302585	2.68939

Since the lines had their own full width half maximum (fwhm) values, this difference needed to be accounted for. Using IRAF, the strong Si line at  $1555.933\mu m$  and the OH line at  $1555.690\mu m$  were measured since they are strong and easily identifiable lines. The two values of fwhm were then averaged to give an estimated fit.

#### 4.3. Abundance Measurements

The next step, and main step of the whole project, was to fit the model parameters to the data. The six elements of Carbon, Nitrogen, Oxygen, Silicon, Titanium, and Iron were used to obtain abundances. However, Carbon was never ultimately altered because any slight alteration in its abundance would alter the molecular composition of the model and drastically change the rest of the model. Nitrogen was fit up to a maximum value of 1.5, for after that, the molecular composition was again altered. For the OH lines, Oxygen was the only element that was altered. Since the stars were almost all hydrogen, changing the hydrogen abundance would really do nothing, Hydrogen was not used and instead Oxygen was used. Silicon and Titanium were altered to fit their one and only line present in the spectrum. Iron was also careful fit due to its importance on the calculation of age due to the metal poor state of the stars. As a result, iron abundance is the main comparison of elements in stars.

### 5. Discussion

Final analysis of the stars were used using the model that had a log g of .5, mass of 1, and microturbulent velocity of 2. This model had all of

its parameters closest to the parameters that were calculated and the fits were best than the other atmospheres.

#### 5.1. Nitrogen Abundances

The Nitrogen abundances were consistent throughout all six of the stars. Each star had a OHCN line stronger than the model. Since carbon and hydrogen were not analyzed for there chemical abundances directly, and since the fitting of oxygen had little effect on this line, this line was mainly effected by Nitrogen. However, as stated earlier, the Nitrogen abundance was not fitted to more than 1.5 so as to eliminate molecular composition change. On two of the stars, the OHCN was fitted almost properly with the corresponding changes of Nitrogen and Oxygen. However, in the other four stars, the line was not even close to being accurately fitted. As a result, either there is a strong, unknown composition at that line, or more likely, the line list that was used in MOOG did not have accurate information on that particular line.

#### 5.2. Oxygen Abundances

Oxygen Abundances varied by star. In some stars, the OH lines fit the model either as a good fit or one too strong. In the other stars, the OH lines were drastically smaller than the data and thus the Oxygen abundances had to be increased.

#### 5.3. Silicon Abundances

The Silicon line was the strongest line and subsequently the strongest element in the stars. It was overall consistent through the stars, and in only one

case, was the line on the same strength as other lines and not noticeably stronger. As a result, in all of the stars, there is a high silicon abundance. This is unusual, however not uncommon. The Silicon line is stronger in the spectrum than the other lines, but do to the metal poor state of the stars, it was even stronger.

#### 5.4. Titanium Abundances

Like the Silicon line, the Titanium line was also much stronger than all the other lines. While the Titanium abundance was noticeably weaker, it still followed the same trend as the Silicon abundance, for in once case, the line was the same strength as the other lines, or more similar than in the other stars. However, in the case of Titanium, the line was stronger than the other lines and the results have shown this. The Titanium abundances in these six stars are stronger than in other comparably similar stars.

#### 5.5. Iron Abundances

Iron had the most influence as to the overall fit of the model. Since there are numerous Iron lines, most of which are small, they still need to be uniquely fit. Thus, Iron was the most critical elemental abundance. Iron, the element that was the main objective of this project, was also the most suprising element. While the iron abundances were stronger than the models and as a result had to be increased, they were are all similar, and yet all significantly weaker than Iron abundances in similar stars. While Silicon and Titanium were stronger in these stars than other stars, Iron was weaker than other, similar stars.

### 6. Conclusions

Careful analysis of six red giants stars in NGC 2019, a globular cluster in the LMC, using infrared spectroscopy, the elemental abundances obtained [Fe/H], [O/H], [Ti/H], and [Si/H] measurements.

The Silicon abundances are high, with abundances at a mean of about 0 and Silicon - Iron abundances about 1.5 The only Silicon line in the spectrum was a blend with OH. Taking into account the abundances of Oxygen, the abundances of Silicon are still strong. This is probably due to an irregular blending at that line and thus inconclusive results.

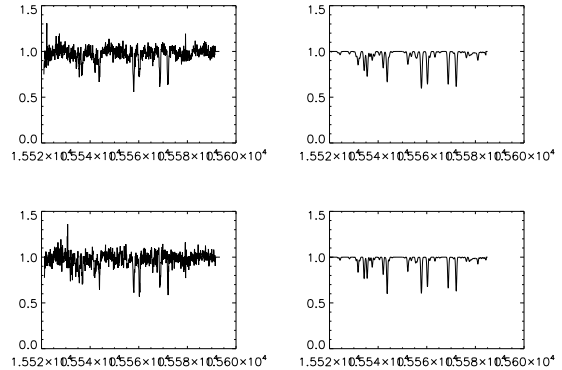


Fig. 3.— Spectrum with fitted models of stars 1 and 3

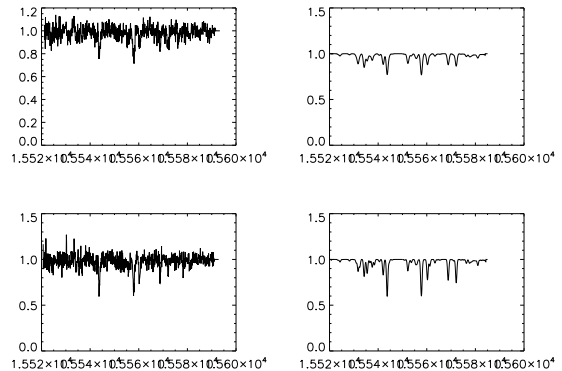


Fig. 4.— Spectrum with fitted models of stars 4 and 6

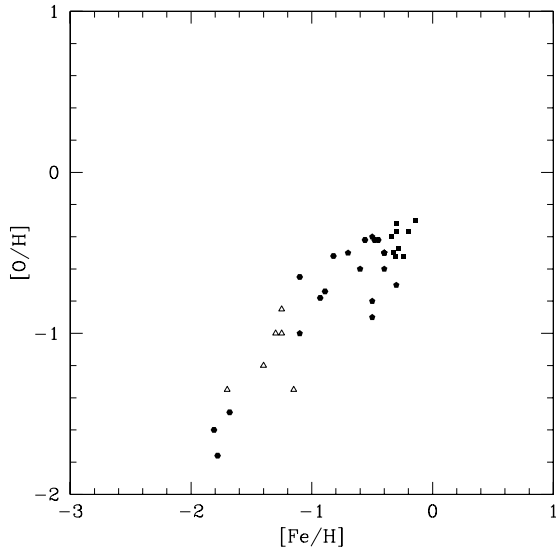


Fig. 5.— Oxygen abundances versus Iron abundances with our data, empty triangle, against other LMC studies

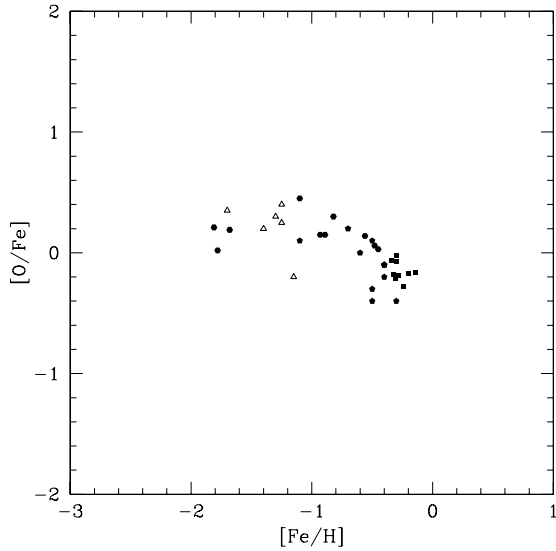


Fig. 6.— Oxygen - Iron versus Iron abundances with our data, empty triangle, against other LMC studies

The Titanium - Iron abundances are higher than those previously measured in other LMC stars. The abundances we obtained are ones that are more similar to abundances found in Globular Clusters towards the outer edges of the Milky Way galaxy.

The Oxygen - Iron abundances measured in NGC 2109 are again more towards those found in the Milky Way galaxy. The abundances show that they have reached a limit in their chemical evolution, equating to abundances no more than .25, a little lower than that of the Milky Way, but closer than previous studies.

The Nitrogen abundances were also interesting.

Data was also taken of NGC 2005, another globular cluster in the LMC. As such, the same process will be analyzed on that globular cluster to see how that compares to the abundances from NGC 2019 and the Milky Way.

TABLE 7  
ABUNDANCE MEASUREMENTS

Model <sup>a</sup>	Star	Nitrogen	Oxygen	Silicon	Titanium	Iron
.5,1,2	1	0.00	-1.10	0.10	-0.70	-1.25
0,.5,2	1	0.00	-1.10	-0.10	-0.80	-1.50
0,1,2	1	0.00	-0.80	0.10	-0.60	-1.25
0,2,2	1	0.00	-0.80	0.10	-0.60	-0.75
0,2,5	1	-0.50	-1.10	-0.10	-0.80	-1.50
0,5,2	1	-0.00	-0.80	0.00	-0.35	-1.00
0,5,5	1	0.00	-0.90	-0.30	-0.60	-1.50
.5,1,5	1	0.00	-1.10	0.10	-0.70	-1.25
.5,1,2	2	-0.50	-0.85	0.15	-0.35	-1.25
0,.5,2	2	-0.50	-0.85	0.15	-0.35	-1.25
0,1,2	2	-0.50	-0.80	-0.40	-0.35	-1.00
0,2,2	2	-0.50	-0.60	-0.35	-0.30	-1.10
0,2,5	2	-0.50	-0.90	-0.30	-0.45	-1.00
0,5,2	2	-0.50	-0.60	-0.25	-0.10	-0.75
0,5,5	2	-0.50	-0.60	-0.25	-0.10	-0.75
.5,1,5	2	-0.50	-0.90	-0.30	-0.45	-1.00
.5,1,2	3	-0.65	-1.00	-0.20	-0.60	-1.25
0,.5,2	3	0.00	-1.10	-0.10	-0.70	-1.50
0,1,2	3	0.00	-1.10	-0.10	-0.60	-1.50
0,2,2	3	-0.50	-1.10	-0.10	-0.60	-1.00
0,2,5	3	-0.50	-1.10	-0.60	-0.80	-1.20
0,5,2	3	-0.50	-1.10	-0.10	-0.60	-1.20
0,5,5	3	-0.50	-1.10	-0.60	-0.80	-1.20
.5,1,5	3	-0.50	-1.10	-0.40	-0.80	-1.25
.5,1,2	4	-0.65	-1.35	-0.10	-0.60	-1.70
0,.5,2	4	-1.50	-1.35	-0.10	-0.70	-1.35
0,1,2	4	-0.50	-1.35	-0.10	-0.70	-1.25
0,2,2	4	-0.50	-1.45	0.00	-0.60	-1.30
0,2,5	4	-0.70	-1.35	-0.20	-0.70	-1.25
0,5,2	4	-0.25	-0.90	-0.30	-0.60	-1.15
0,5,5	4	-0.50	-1.35	-0.20	-0.70	-1.20
.5,1,5	4	-0.50	-1.35	-0.10	-0.60	-1.25
.5,1,2	5	-0.75	-1.35	-0.10	-0.90	-1.15
0,.5,2	5	-0.50	-1.35	-0.10	-1.20	-1.00
0,1,2	5	-0.25	-1.30	-0.10	-1.10	-1.10
0,2,2	5	-0.20	-1.35	-0.35	-1.10	-1.00
0,2,5	5	-0.60	-1.35	-0.45	-1.10	-1.20
0,5,2	5	-0.50	-1.35	-0.10	-1.10	-1.00
0,5,5	5	-0.50	-1.35	-0.45	-1.10	-1.20
.5,1,5	5	-0.50	-1.30	-0.45	-1.10	-1.15
.5,1,2	6	-0.65	-1.20	0.50	-0.10	-1.40
0,.5,2	6	-0.25	-1.35	0.45	-0.35	-1.15
0,1,2	6	-0.65	-1.25	0.25	-0.35	-1.00
0,2,2	6	-0.50	-1.25	0.30	-0.35	-1.20
0,2,5	6	-0.70	-1.20	-0.15	-0.55	-1.25
0,5,2	6	-0.75	-1.25	0.25	-0.30	-1.00

TABLE 7—*Continued*

Model <sup>a</sup>	Star	Nitrogen	Oxygen	Silicon	Titanium	Iron
0,5,5	6	-0.75	-1.30	-0.10	-0.50	-1.25
.5,1,5	6	-0.75	-1.35	-0.10	-0.60	-1.25

<sup>a</sup>Model in terms of log of gravity, mass, and microturbulent velocity